Pyridinium-1-yl Bisphosphonates Are Potent Inhibitors of Farnesyl Diphosphate Synthase and Bone Resorption

John M. Sanders,[†] Yongcheng Song,[†] Julian M. W. Chan,[†] Yonghui Zhang,[†] Samuel Jennings,[†] Thomas Kosztowski,[†] Sarah Odeh,[†] Ryan Flessner,[†] Christine Schwerdtfeger,[†] Evangelia Kotsikorou,[†] Gary A. Meints,[†] Aurora Ortiz Gómez,[‡] Dolores González-Pacanowska,[‡] Amy M. Raker,[§] Hong Wang,[§] Ermond R. van Beek,[∥] Socrates E. Papapoulos,[∥] Craig T. Morita,[§] and Eric Oldfield*[,†,⊥]

Department of Chemistry, 600 South Mathews Avenue, University of Illinois at Urbana-Champaign, Urbana, Illinois 61801; López-Neyra Institute of Parasitology and Biomedicine, CSIC, Granada, Spain; Department of Internal Medicine and the Interdisciplinary Group in Immunology, University of Iowa, EMRB 340F, Iowa City, Iowa 52242; Department of Endocrinology and Metabolic Diseases, Leiden University Medical Center, Leiden, The Netherlands; and Department of Biophysics, 600 South Mathews Avenue, University of Illinois at Urbana-Champaign, Urbana, Illinois 61801

Received December 3, 2004

We report the design, synthesis and testing of a series of novel bisphosphonates, pyridinium-1-yl-hydroxy-bisphosphonates, based on the results of comparative molecular similarity indices analysis and pharmacophore modeling studies of farnesyl diphosphate synthase (FPPS) inhibition, human Vγ2Vδ2 T cell activation and bone resorption inhibition. The most potent molecules have high activity against an expressed FPPS from *Leishmania major*, in *Dictyostelium discoideum* growth inhibition, in $\gamma\delta$ T cell activation and in an in vitro bone resorption assay. As such, they represent useful new leads for the discovery of new bone resorption, antiinfective and anticancer drugs.

Introduction

Nitrogen-containing bisphosphonates such as pamidronate (Aredia, **1**), alendronate (Fosamax, **2**), risedronate (Actonel, **3**) and zoledronate (Zometa, **4**), shown below in their zwitterionic forms, represent an important class of drugs currently used to treat osteoporosis, Paget's disease and hypercalcemia due to malignancy.[1−4] These compounds function primarily by adsorbing to bone and inhibiting the enzyme farnesyl diphosphate synthase (FPPS) in osteoclasts,[5−12] resulting in decreased levels of protein prenylation.[13−15] Bisphosphonates have also been found to have anti-parasitic activity,[16−25] and have been found to stimulate human $\gamma\delta$ T cells,[26−30] where there is currently interest in their use as vaccines for a variety of B cell malignancies.[31] Given their proven clinical utility, there is interest in their further development.

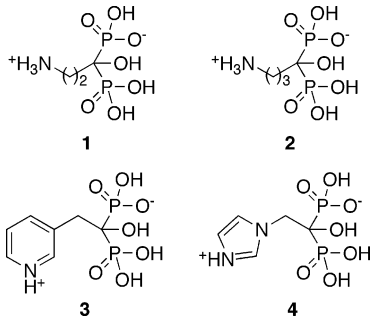

In recent work, we carried out a series of quantitative structure−activity relationship (QSAR) studies of the activity of bisphosphonates in FPPS inhibition,[17] Vγ2Vδ2 T cell activation[30] and bone resorption[32] using comparative molecular field analysis (CoMFA),[33] comparative molecular similarity indices analysis (CoMSIA)[34] and pharmacophore modeling[35] approaches. An interesting result emerging from these studies was that the CoMSIA field maps for the hydrophobic, electrostatic and steric fields found for FPPS inhibition by bisphosphonates were similar to the CoMSIA field maps found for bisphosphonates acting as $\gamma\delta$ T cell stimulators and in bone resorption.[17,30,32] Likewise, the pharmacophore models for the inhibition of recombinant human FPPS were very similar to those found for stimulation of $\gamma\delta$ T cells by bisphosphonates,[30] and the pIC_{50}/pEC_{50} results for FPPS inhibition and Vγ2Vδ2 T cell stimulation were highly correlated ($R = 0.89$, $p = 0.0012$).[30] All of these CoMSIA and pharmacophore modeling investigations clearly showed the importance of the presence of a positive charge feature at a relatively localized position in the bisphosphonate side chain. This feature can, of course, be related to the position of the positive charge feature expected in the pyridinium and imidazolium forms of **3** and **4**, shown above, and is centered close to the bisphosphonate backbone. This suggested to us that pyridinium-1-yl species, such as **5**, might have enhanced

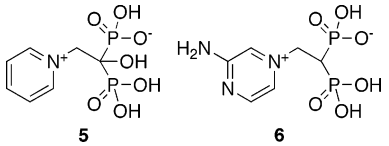

* To whom correspondence should be addressed. Telephone: (217) 333-3374. Fax: (217) 244-0997. E-mail: eo@chad.scs.uiuc.edu.
[†] Department of Chemistry, University of Illinois at Urbana-Champaign.
[‡] López-Neyra Institute of Parasitology and Biomedicine.
[§] University of Iowa.
[∥] Leiden University Medical Center.
[⊥] Department of Biophysics, University of Illinois at Urbana-Champaign.

10.1021/jm040209d CCC: $30.25
Published on Web 03/08/2005

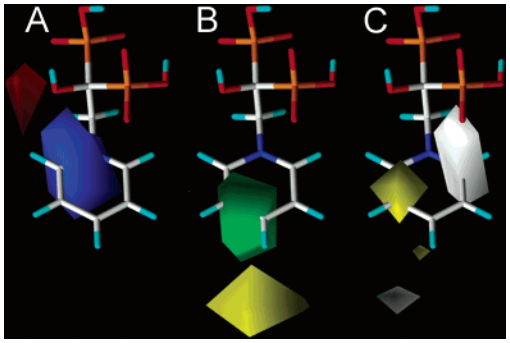

Figure 1. *L. major* FPPS CoMSIA fields (from ref 17) superimposed on **5**. A, electrostatic field (blue region = positive charge enhances activity, red region = positive charge detracts from activity); B, steric field (green regions = steric feature enhances activity, yellow regions = steric feature detracts from activity); C, hydrophobic field (yellow region = hydrophobic feature enhances activity, white region = hydrophobic feature detracts from activity).

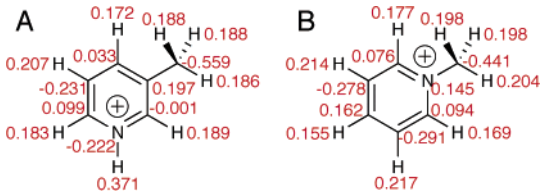

Figure 2. Charge distributions in the side chains of **3** (A) and **5** (B). The numbers represent Merz−Singh−Kollman charges[39,40] evaluated using the Gaussian 03 program.[38] The side chains of **3** and **5** were geometry optimized using the Hartree−Fock method with a uniform 6-31G* basis set and these optimized geometries were used in the atomic charge calculations.

activity, and indeed in previous work several other groups have reported the synthesis of a variety of analogues of **5** which lack the 1-OH group, such as **6**.[36] However, these compounds might not be expected to be effective in bone resorption, since they lack the "bone hook" feature identified in CoMSIA fields[32] and in other studies.[37] We therefore undertook the synthesis of **5** and a series of derivatives, all containing the 1-OH feature, and we discuss here their activities in FPPS inhibition, $\gamma\delta$ T cell activation, *Dictyostelium discoideum* growth inhibition (a model for bone resorption) and in an in vitro bone resorption assay.

Results and Discussion

We show in Figure 1 the CoMSIA fields for *L. major* FPPS inhibition[17] superimposed on the structure of **5**. The pyridinium-1-yl nitrogen in **5** (1-hydroxy-2-(pyridinium-1-yl)ethylidene-1,1-bisphosphonic acid) can be seen to be located in the blue CoMSIA field region, where positive charge enhances activity. The results of quantum chemical calculations[38] of the truncated side chains of **3** and **5** show, as expected, that there are relatively large positive charges on the nitrogen and adjacent C, H atoms in this region, as can be seen in the Merz−Singh−Kollman charges[39,40] (Figure 2). These results indicate that **5** should contain considerably more positive charge than does **3** in the region identified by the CoMSIA electrostatic field (Figure 1A) and might contribute to enhanced activity. We therefore synthesized the hydroxy species, **5**, and a series of derivatives (**7**−**18**, Figure 3), all of which contain the 1-OH feature, using the following general scheme:

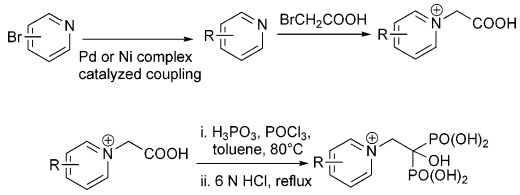

In the first step, we used (where necessary) coupling reactions of arylmetallic compounds with bromopyridines, catalyzed by $Pd(PPh_3)_4$[41] or $NiCl_2(PPh_3)_2$,[42] to produce substituted pyridines. The substituted pyridines were then alkylated by using bromoacetic acid,[43] and the resulting pyridinium-1-yl acetic acids were converted to the corresponding bisphosphonates by using $H_3PO_3/POCl_3$.[44] Next, we investigated the activity of each compound in inhibiting the FPPS from *L. major*, in *Dictyostelium discoideum* growth inhibition, in $\gamma\delta$ T cell activation, and, for a subset of compounds, in bone resorption. We used the FPPS from *L. major,* since FPPS is the putative bisphosphonate target in several trypanosomatid species, and the *L. major* FPPS was the enzyme previously used to establish the initial QSAR models.[17] We used *D. discoideum* to test for cell growth inhibition, since this organism has been used previously in the context of the development of bone resorption drugs.[45] To determine the stimulatory activity of **5** and **7**−**18** for Vγ2Vδ2 T cells, we used the TNF-α release assay described previously,[30] and for the bone resorption assay, we used the 17-day old fetal mouse metatarsal $^{45}Ca^{2+}$ release assay described elsewhere.[46]

In the *L. major* FPPS inhibition assay, **5** was found to have a K_i of 18 nM (Table 1) and was thus slightly less active than the most potent commercially available bisphosphonates, zoledronate (**4**, K_i = 11 nM, in this assay) and risedronate (**3**, K_i = 17 nM, in this assay) (Table 1). To try to enhance activity, we next inspected the steric and hydrophobic CoMSIA fields for FPPS inhibition (Figures 1B and 1C, respectively), which suggested the desirability of placing an additional steric and hydrophobic feature at the meta position. We thus prepared compounds **7**−**9** (Figure 3) and tested them in the FPPS assay. The *m*-methyl analogue of **5** (**7**) was not as active as **5** (K_i = 38 nM versus 18 nM), but substitution with a *m*-phenyl group, giving **8**, resulted in a very potent species, having a K_i = 9 nM, slightly more active than zoledronate, **4** (K_i = 11 nM). The *p*-phenoxy derivative of **5** (**9**) was found to be less active (K_i = 75 nM), possibly due to unfavorable electrostatic interactions of the OH group in the FPPS active site. Since the phenylpyridinium species, **8**, displayed good activity, we next synthesized **10** and **11**. Both of these compounds contain a methylene linker between the two aromatic groups, and it seemed possible that they might better mimic the putative geranyl diphosphate reactive intermediate (**19**), but each of these compounds was less

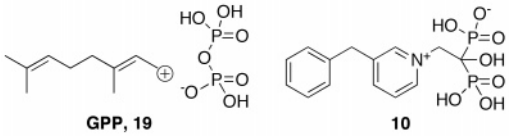

active than **8,** with K_is in the 70−160 nM range, Table

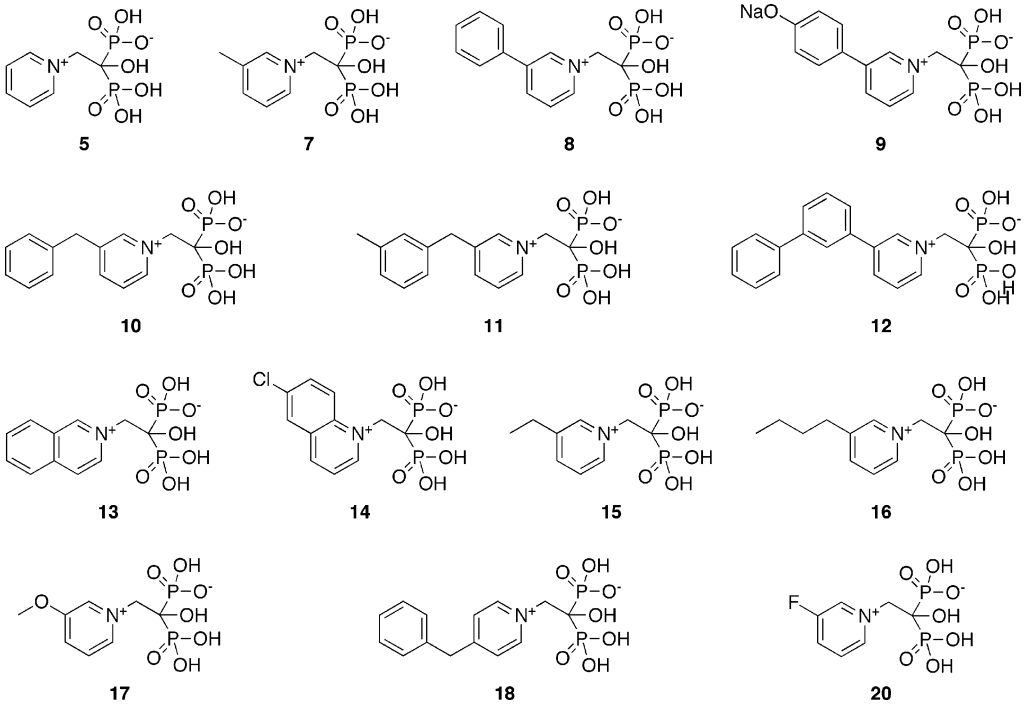

Figure 3. Structures of pyridinium-1-yl bisphosphonates.

Table 1. Activities of Bisphosphonates as *L. Major* FPPS Inhibitors, *D. Discoideum* Cell Growth Inhibitors, $\gamma\delta$ T Cell Simulators and Bone Resorption Agents

compound	*L. major* FPPS K_i (nM)	*D. discoideum* IC_{50} (μM)	$\gamma\delta$ T cell stimulation EC_{50} (μM)	in vitro bone resorption IC_{50} (μM)
1 (pamidronate)[a,b]	190	167	43	1.6
2 (alendronate)[a,b]	95	32	32	0.29
3 (risedronate)[a,b]	17	3.0	5.0	0.30
4 (zoledronate)[a,b]	11	2.9	5.4	0.034
5	18	2.1	4.8	0.67
7	38	1.5	4.5	0.22
8	9	3.8	4.1	0.41
9	75	2.9	2.5	N.D.[c]
10	160	11	91	N.D.
11	70	9.2	44	N.D.
12	950	2.3	inactive	N.D.
13	80	20	30	N.D.
14	380	72	56	N.D.
15	20	5.6	4.4	N.D.
16	20	2.9	4.3	N.D.
17	30	6.0	9.3	0.37
18	110	12	150	N.D.
20	50	4.6	2.7	0.075

[a] *L. major* FPPS inhibition data from ref 17. [b] Data averaged over unconstrained $\gamma\delta$ T cell stimulation data from ref 30 and data obtained since publication of ref 30. [c] N.D. = not determined.

1. We also prepared the biphenylpyridinium compound, **12**, since the added hydrophobicity of **8** appeared encouraging, but **12** proved to be relatively inactive, having a K_i of 950 nM. Enhancing the size of the hydrophobic/steric feature by use of isoquinoline and quinoline side chains, **13** and **14**, resulted in modest activity (80 and 380 nM, respectively, for **13** and **14**), but the *m*-ethyl (**15**), -butyl (**16**), -methoxy (**17**) and *p*-benzyl (**18**) pyridinium species were generally more active (20, 20, 30 and 110 nM, respectively), although they were less active than **3**−**5**, **8**, Table 1.

We next investigated *D. discoideum* growth inhibition by **1**−**5** and **7**−**18** (Table 1). The most active compound found was the *meta*-methyl pyridinium compound, **7**, which had an IC_{50} of 1.5 μM, followed by the unsubstituted pyridinium bisphosphonate, **5**, which was slightly more active (IC_{50} = 2.1 μM) than was risedronate (**3**, IC_{50} = 3.0 μM) and zoledronate (**4**, IC_{50} = 2.9 μM). As with the FPPS inhibition results, the benzylpyridinium bisphosphonates (**10**, **11**, **18**) were less active than the pyridinium and phenylpyridinium species (**5**, **7**−**9**). Surprisingly, **12** showed high activity (IC_{50} = 2.3 μM), due perhaps to the possibility of an additional target in *D. discoideum* or the possibility of structural differences between *L. major* and *D. discoideum* FPPSs. With the exception of **12**, the activity results for the 17 bisphosphonates were found to be correlated (R^2 = 0.61, p = 0.0002) with the *L. major* FPPS inhibition activities, as shown in Figure 4A.

Next, we investigated the ability of **5** and **7**−**18** to stimulate $\gamma\delta$ T cells, using the TNF-α release assay and the unconstrained fitting procedure described previously.[30] The most active compound was found to be **8** (EC_{50} = 4.1 μM), followed by **16** (EC_{50} = 4.3 μM),

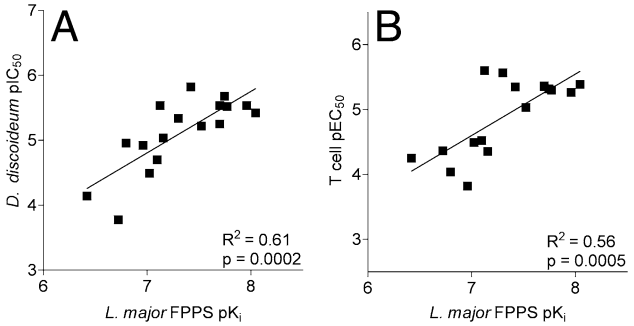

Figure 4. Graphs showing correlations between FPPS inhibition and A, *D. discoideum* growth inhibition and B, $\gamma\delta$ T cell activation (as determined by TNF-α release). The R^2 and p values are $R^2 = 0.61$ and $p = 0.0002$ in A and $R^2 = 0.56$ and $p = 0.0005$ in B.

15 (EC_{50} = 4.4 μM), **7** (EC_{50} = 4.5 μM) and **5** (EC_{50} = 4.8 μM), with these compounds having more activity than risedronate (**3**, EC_{50} = 5.0 μM) or zoledronate (**4**, EC_{50} = 5.4 μM) in this TNF-α release assay. Addition of the *p*-hydroxyl group (**8** → **9**) decreased the EC_{50} slightly (Table 1), but **9** did not display the maximal TNF-α release achieved with risedronate. All three methylene-bridged compounds (**10**, **11**, **18**) had poor activity, as in the other assays investigated. The activity results for FPPS inhibition were found to be correlated with the $\gamma\delta$ T cell TNF-α release results (R^2 = 0.56, p = 0.0005), as shown in Figure 4B, suggesting once again the likely importance of FPPS inhibition in $\gamma\delta$ T cell activation.[29,30]

Finally, we tested a subset of these compounds (**1**, **2**, **3**, **4**, **5**, **7**, **8** and **17**) in a bone resorption assay: $^{45}Ca^{2+}$ release from 17-day old fetal mouse metatarsals.[46] Results for pamidronate (**1**), alendronate (**2**), risedonate (**3**), zoledronate (**4**), **5**, **7**, **8** and **17** are shown in Figure 5A and yielded IC_{50} values of 1.6 μM (**1**), 290 nM (**2**), 300 nM (**3**), 34 nM (**4**), 670 nM (**5**), 220 nM (**6**), 410 nM (**8**) and 370 nM (**17**), Figure 5B. So the pyridinium bisphosphonates studied are all more active in this bone resorption assay than is pamidronate, with **7** showing slightly higher activity than alendronate and risedronate.

In an effort to improve upon these promising bone resorption results, we synthesized the 3-fluoro analogue of **5**, **20**, since the electron-withdrawing nature of this fluorine would be expected to increase the amount of positive charge on the ring. When tested in the *L. major* FPPS assay, **20** was found to have a K_i of 50 nM, and in the *D. discoideum* inhibition assay, we found an IC_{50} = 4.6 μM. In both cases, then, there was a decrease in activity. However, when tested in the human $\gamma\delta$ T cell activation assay, we found a slight increase in activity on fluorine substitution (from 4.8 μM with **5** to 2.7 μM with **20**), and in the bone resorption assay the effect was much larger, with a 75 nM IC_{50} for **20** (Figure 5) to be compared with a 670 nM IC_{50} for **5**, Table 1. These results show, therefore, that **20** is more active in this bone resorption assay than the drugs currently used to treat osteoporosis, alendronate (**2**, IC_{50} = 290 nM) and risedronate (**3**, IC_{50} = 300 nM), although it is less active than zoledronate (**4**, IC_{50} = 34 nM).

Overall, the results presented above are of interest since they represent the first report of the QSAR-based design,[17,30] synthesis and testing of a series of novel pyridinium-1-yl hydroxy-bisphosphonates for activity against a farnesyl diphosphate synthase, *D. discoideum* growth inhibition, human $\gamma\delta$ T cell activation, and in bone resorption. In each of the four assays, pyridinium-1-yl bisphosphonates having high activity have been found, suggesting that the further development of this class of compounds may be of interest in the context of the chemotherapy of infectious diseases, in bone resorption, and in immunotherapy.

Experimental Section

Synthetic Aspects. There are two basic steps to produce the pyridinium-1-yl bisphosphonates: (1) synthesis of the parent pyridine (when not commercially available), using either $Pd(PPh_3)_4$ catalyzed (Suzuki) coupling of an arylboronic acid and bromopyridine[41] or, in the case of **11**, $NiCl_2(PPh_3)_2$-catalyzed coupling of a benzyl zinc compound and bromopyridine;[42] (2) carboxymethylation of the (substituted) pyridine with bromoacetic acid[43] followed by phosphorylation of the resulting pyridinium-1-yl acetic acids with $POCl_3/H_3PO_3$.[44] Full details of the synthesis of each compound are given below, and, in most cases (i.e. except for **11**), the syntheses followed both of the following two general procedures. Purity of products was established via C/H/N microanalysis and 500 MHz ^1H NMR spectroscopy.

General Procedure 1: Preparation of Aryl-Substituted Pyridines. A mixture of an aryl boronic acid or its ester (3 mmol), 3-bromopyridine (3 mmol), $Pd(PPh_3)_4$ (0.075 mmol), K_2CO_3 (1.2 g, 9 mmol), toluene (12 mL) and H_2O (3 mL) was refluxed for 10 h.[41] The product was extracted with Et_2O and purified by using silica gel chromatography.

General Procedure 2: Preparation of 1-Hydroxy-2-(substituted-pyridinium-1-yl)ethylidene-1,1-bisphosphonic Acids. Bromoacetic acid (2 mmol) was added to a solution of substituted pyridine (2 mmol) in ethyl acetate (3 mL) and the reaction mixture stirred at room temperature for 2 days, giving the substituted 1-carboxymethylpyridinium bromide as a white precipitate. This was then filtered, washed with ethyl acetate (2 × 3 mL) and dried in vacuo. The resulting white powder was added to a mixture of H_3PO_3 (5 equivalents) and toluene (6 mL) and heated to 80 °C, with stirring. After all solids had melted, $POCl_3$ (5 equiv) was added dropwise and the reaction mixture vigorously stirred at 80 °C for 5 h. Upon cooling, the supernatant was decanted and 6 N HCl (3 mL) added to the residue. The resulting solution was refluxed for 1 h, then most of the solvent was removed in vacuo. 2-Propanol (25 mL) was added to precipitate the title compounds as white powders. These were filtered, washed with 2-propanol (5 × 5 mL) then dried and were further purified by recrystallization from H_2O/2-PrOH. In some cases, oily products were neutralized with NaOH, then crystallized as the sodium salts from H_2O/2-PrOH.

1-Hydroxy-2-(pyridinium-1-yl)ethylidene-1,1-bisphosphonic Acid (5). **5** was prepared from pyridine (395 mg, 5 mmol) following general procedure 2 (960 mg, 68% overall yield). Anal. ($C_7H_{11}NP_2O_7$) C, H, N. ^1H NMR (400 MHz, D_2O): δ 4.87 (t, J_{PH} = 7.2 Hz, 2H, CH_2), 7.84 (t, J_{HH} = 5.6 Hz, 2H, aromatics), 8.38 (t, J_{HH} = 5.6 Hz, 1H, aromatics), 8.71 (d, J_{HH} = 5.6 Hz, 2H, aromatics); ^{31}P NMR (162 MHz, D_2O): δ 14.3 (s).

1-Hydroxy-2-(3-methylpyridinium-1-yl)ethylidene-1,1-bisphosphonic Acid (7). **7** was prepared from 3-methylpyridine (465 mg, 5 mmol) following general procedure 2 (850 mg, 57% overall yield). Anal. ($C_8H_{13}NP_2O_7$) C, H, N. ^1H NMR (400 MHz, D_2O): δ 2.36 (s, 3H, CH_3), 4.67 (t, J_{PH} = 8.0 Hz, 2H, CH_2), 7.68 (t, J_{HH} = 6.4 Hz, 1H, aromatics), 8.16 (d, J_{HH} = 6.4 Hz, 1H, aromatics), 8.50 (d, J_{HH} = 6.4 Hz, 1H, aromatics), 8.53 (s, 1H, aromatics); ^{31}P NMR (162 MHz, D_2O): δ 14.1 (s).

1-Hydroxy-2-(3-phenylpyridinium-1-yl)ethylidene-1,1-bisphosphonic Acid (8). **8** was prepared from 3-phenylpyridine (310 mg, 2 mmol) following general procedure 2 as the disodium salt (570 mg, 65% overall yield). Anal.

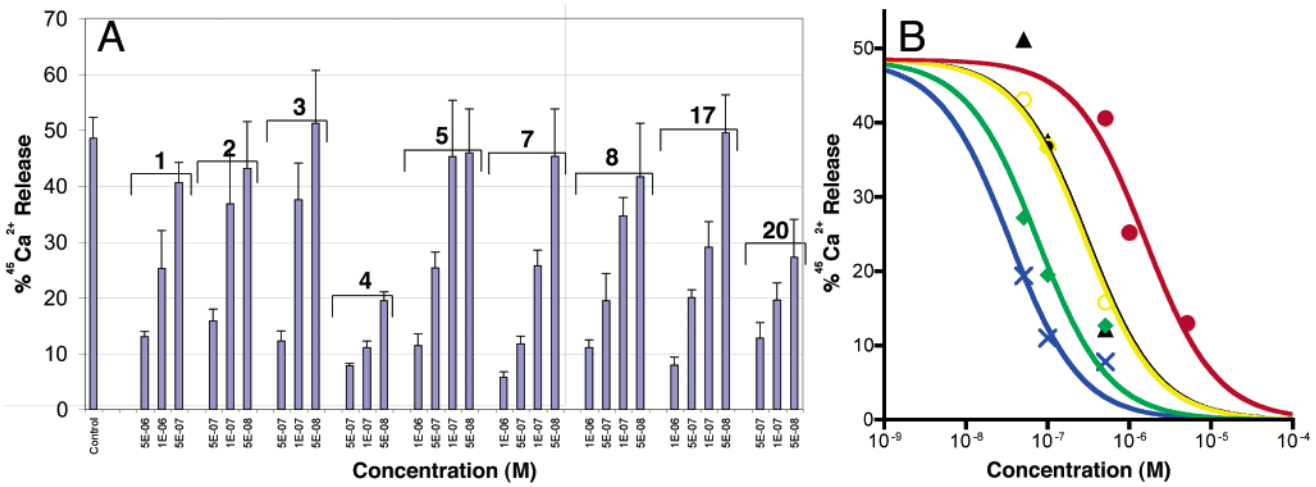

Figure 5. A, $^{45}Ca^{2+}$ release from 17-day old fetal mouse metatarsals[46] for control and compounds **1**, **2**, **3**, **4**, **5**, **7**, **8**, **17** and **20.** The braces delineate bone resorption data sets and compound numbers. B, Dose−response curves for **1** (●), **2** (○), **3** (▲), **4** (×) and **20** (◆).

($C_{13}H_{13}NP_2O_7Na_2 \cdot 2\ H_2O$) C, H, N. ^1H NMR (400 MHz, D_2O): δ 4.75 (t, J_{PH} = 8.0 Hz, 2H, CH_2), 7.30−7.40 (m, 3H, aromatics), 7.50−7.60 (m, 2H, aromatics), 7.68 (t, J_{HH} = 5.6 Hz, 1H, aromatics), 8.39 (d, J_{HH} = 5.6 Hz, 1H, aromatics), 8.60 (d, J_{HH} = 5.6 Hz, 1H, aromatics), 8.91 (s, 1H, aromatics); ^{31}P NMR (162 MHz, D_2O): δ 14.3 (s).

1-Hydroxy-2-[3-(4-hydroxyphenyl)pyridinium-1-yl]ethylidene-1,1-bisphosphonic Acid (9). **9** was prepared from 4-(4,4,5,5-tetramethyl-1,3-dioxaborolan-2-yl)phenyl acetate (786 mg, 3 mmol) following general procedures 1 and 2 as a tetrasodium salt (620 mg, 40% overall yield). Anal. ($C_{13}H_{11}NP_2O_8Na_4 \cdot 3\ H_2O$) C, H, N. ^1H NMR (400 MHz, D_2O): δ 4.83 (t, J_{PH} = 8.0 Hz, 2H, CH_2), 6.74 (d, J_{HH} = 6.8 Hz, 2H, aromatics), 7.49 (d, J_{HH} = 6.8 Hz, 2H, aromatics), 7.77 (t, J_{HH} = 6.0 Hz, 1H, aromatics), 8.45 (d, J_{HH} = 6.0 Hz, 1H, aromatics), 8.55 (d, J_{HH} = 6.0 Hz, 1H, aromatics), 8.89 (s, 1H, aromatics); ^{31}P NMR (162 MHz, D_2O): δ 14.6 (s).

1-Hydroxy-2-(3-benzylpyridinium-1-yl)ethylidene-1,1-bisphosphonic Acid (10). **10** was prepared from 3-benzylpyridine (340 mg, 2 mmol) following general procedure 2 as a trisodium salt (560 mg, 60% overall yield). Anal. ($C_{14}H_{14}NP_2O_7Na_3 \cdot 1.5\ H_2O$) C, H, N. ^1H NMR (400 MHz, D_2O): δ 4.07 (s, 2H, $PhCH_2$), 4.76 (t, J_{PH} = 9.2 Hz, 2H, NCH_2), 7.10−7.25 (m, 5H, aromatics), 7.69 (t, J_{HH} = 6.8 Hz, 1H, aromatics), 8.14 (d, J_{HH} = 6.8 Hz, 1H, aromatics), 8.54 (d, J_{HH} = 6.8 Hz, 1H, aromatics), 8.58 (s, 1H, aromatics); ^{31}P NMR (162 MHz, D_2O): δ 13.9 (s).

1-Hydroxy-2-[3-(3-methylbenzyl)pyridinium-1-yl]ethylidene-1,1-bisphosphonic Acid (11). 3-(3-Methylbenzyl)-pyridine was prepared by a published method.[42] In brief, 3-methylbenzyl bromide (0.88 mL, 6.5 mmol) and Zn powder (0.55 g, 8.5 mmol) in THF (6 mL) were stirred for 2 h at room temperature, and the supernatant solution transferred to a THF solution (6 mL) containing 3-bromopyridine (0.49 mL, 5 mmol) and $NiCl_2(PPh_3)_2$ (654 mg, 1 mmol). The reaction mixture was stirred at room-temperature overnight before quenching with 10% ammonia. The product was extracted with Et_2O and purified by column chromatography (silica gel, Et_2O/hexane 1:1, 86% yield). The title compound **11** was prepared from 3-(3-methylbenzyl)pyridine (370 mg, 2 mmol) following general procedure 2 as a trisodium salt (700 mg, 70% overall yield). Anal. ($C_{15}H_{16}NP_2O_7Na_3 \cdot 2.5\ H_2O$) C, H, N. ^1H NMR (400 MHz, D_2O): δ 2.15 (s, 3H, CH_3), 4.04 (s, 2H, $PhCH_2$), 4.78 (t, J_{PH} = 7.6 Hz, 2H, NCH_2), 6.90−7.20 (m, 4H, aromatics), 7.70 (t, J_{HH} = 6.0 Hz, 1H, aromatics), 8.15 (d, J_{HH} = 6.0 Hz, 1H, aromatics), 8.55 (d, J_{HH} = 6.0 Hz, 1H, aromatics), 8.59 (s, 1H, aromatics); ^{31}P NMR (162 MHz, D_2O): δ 14.3 (s).

1-Hydroxy-2-[3-(3-biphenyl)pyridinium-1-yl]ethylidene-1,1-bisphosphonic Acid (12). **12** was prepared from 3-biphenyl boronic acid (600 mg, 3 mmol) following general procedures 1 and 2 (750 mg, 56% overall yield). Anal. ($C_{19}H_{19}NP_2O_7 \cdot 0.5\ H_2O$) C, H, N; C: calcd, 51.36; found, 50.94. ^1H NMR (400 MHz, D_2O): δ 4.84 (t, J_{PH} = 8.8 Hz, 2H, CH_2), 7.20−7.80 (m, 10H, aromatics), 8.44 (d, J_{HH} = 6.0 Hz, 1H, aromatics), 8.68 (d, J_{HH} = 6.0 Hz, 1H, aromatics), 8.98 (s, 1H, aromatics); ^{31}P NMR (162 MHz, D_2O): δ 14.0 (s).

1-Hydroxy-2-[isoquinolinium-2-yl]ethylidene-1,1-bisphosphonic Acid (13). **13** was prepared from isoquinoline (400 mg, 3 mmol) following general procedure 2 (486 mg, 47% overall yield). Anal. ($C_{11}H_{13}NP_2O_7 \cdot 0.25\ H_2O$) C, H, N. ^1H NMR (400 MHz, D_2O): δ 4.99 (t, J_{PH} = 8.0 Hz, 2H, CH_2), 7.84 (t, J_{HH} = 5.6 Hz, 1H, aromatics), 8.00−8.10 (m, 2H, aromatics), 8.15 (d, J_{HH} = 5.6 Hz, 1H, aromatics), 8.27 (d, J_{HH} = 5.6 Hz, 1H, aromatics), 8.39 (d, J_{HH} = 5.6 Hz, 1H, aromatics), 9.56 (s, 1H, aromatics); ^{31}P NMR (162 MHz, D_2O): δ 14.2 (s).

1-Hydroxy-2-[6-chloroquinolinium-1-yl]ethylidene-1,1-bisphosphonic Acid (14). **14** was prepared from 6-chloroquinoline (1 g, 6.1 mmol) following general procedure 2 (243 mg, 10% overall yield). Anal. ($C_{11}H_{12}NP_2O_7Cl \cdot H_2O$) C, H, N. ^1H NMR (400 MHz, D_2O): δ 5.33 (t, J_{PH} = 10.0 Hz, 2H, CH_2), 7.80−7.85 (m, 1H, aromatics), 7.95−8.00 (m, 1H, aromatics), 8.15 (s, 1H, aromatics), 8.50 (d, J_{HH} = 5.6 Hz, 1H, aromatics), 8.84 (d, J_{HH} = 5.6 Hz, 1H, aromatics), 9.18 (d, J_{HH} = 5.6 Hz, 1H, aromatics); ^{31}P NMR (162 MHz, D_2O): δ 14.3 (s).

1-Hydroxy-2-[3-ethylpyridinium-1-yl]ethylidene-1,1-bisphosphonic Acid (15). **15** was prepared from 3-ethylpyridine (430 mg, 4 mmol) following general procedure 2 (750 mg, 60% overall yield). Anal. ($C_9H_{15}NP_2O_7$) C, H, N. ^1H NMR (400 MHz, D_2O): δ 1.11 (t, J_{HH} = 7.6 Hz, 3H, CH_3), 2.69 (q, J_{HH} = 7.6 Hz, 2H, CH_2), 4.74 (t, J_{PH} = 8.0 Hz, 2H, NCH_2), 7.68 (t, J_{HH} = 6.4 Hz, 1H, aromatics), 8.17 (d, J_{HH} = 6.4 Hz, 1H, aromatics), 8.50−8.60 (m, 2H, aromatics); ^{31}P NMR (162 MHz, D_2O): δ 14.3 (s).

1-Hydroxy-2-[3-butylpyridinium-1-yl]ethylidene-1,1-bisphosphonic Acid (16). **16** was prepared from 3-butylpyridine (540 mg, 4 mmol) following general procedure 2 (690 mg, 51% overall yield). Anal. ($C_{11}H_{19}NP_2O_7 \cdot 0.25\ H_2O$) C, H, N. ^1H NMR (400 MHz, D_2O): δ 0.72 (t, J_{HH} = 7.2 Hz, 3H, CH_3), 1.10−1.20 (m, 2H, CH_2), 1.45−1.55 (m, 2H, CH_2), 2.67 (q, J_{HH} = 7.2 Hz, 2H, CH_2), 4.79 (t, J_{PH} = 8.0 Hz, 2H, NCH_2), 7.70 (t, J_{HH} = 6.8 Hz, 1H, aromatics), 8.20 (d, J_{HH} = 6.8 Hz, 1H, aromatics), 8.50−8.60 (m, 2H, aromatics); ^{31}P NMR (162 MHz, D_2O): δ 14.3 (s).

1-Hydroxy-2-[3-methoxylpyridinium-1-yl]ethylidene-1,1-bisphosphonic Acid (17). **17** was prepared from 3-methoxypyridine (440 mg, 4 mmol) following general procedure 2 (900 mg, 72% overall yield). Anal. ($C_8H_{13}NP_2O_7 \cdot H_2O$) C, H, N. ^1H NMR (400 MHz, D_2O): δ 3.80 (s, 3H, CH_3), 4.75 (t, J_{PH} = 8.4 Hz, 2H, CH_2), 7.58 (t, J_{HH} = 6.8 Hz, 1H, aromatics), 7.78 (d, J_{HH} = 6.8 Hz, 1H, aromatics), 8.17 (d, J_{HH} = 6.8 Hz, 1H, aromatics), 8.45 (s, 1H, aromatics); ^{31}P NMR (162 MHz, D_2O): δ 14.2 (s).

1-Hydroxy-2-[4-benzylpyridinium-1-yl]ethylidene-1,1-bisphosphonic Acid (18). **18** was prepared from 4-benzylpyridine (380 mg, 2.2 mmol) following general procedure 2 (337 mg, 40% overall yield). Anal. ($C_{14}H_{16}NP_2O_7Na\cdot 0.5\ H_2O$) C, H, N. ^{1}H NMR (400 MHz, D_2O): δ 4.08 (s, 2H, $PhCH_2$), 4.76 (t, $J_{PH} = 9.2$ Hz, 2H, NCH_2), 7.10−7.30 (m, 5H, aromatics), 7.61 (d, $J_{HH} = 6.8$ Hz, 2H, aromatics), 8.46 (d, $J_{HH} = 6.8$ Hz, 2H, aromatics); ^{31}P NMR (162 MHz, D_2O): δ 14.0 (s).

1-Hydroxy-2-[3-fluoropyridinium-1-yl]ethylidene-1,1-bisphosphonic Acid (20). **20** was prepared from 3-fluoropyridine (214 mg, 2.2 mmol) following general procedure 2 (304 mg, 46% overall yield). Anal. ($C_7H_{10}FNP_2O_7$) C, H, N; C: calcd, 28.41; found, 27.92. ^{1}H NMR (400 MHz, D_2O): δ 4.80 (t, $J_{PH} = 8.4$ Hz, 2H, CH_2), 7.80−7.88 (m, 1H, aromatics), 8.15 (t, $J_{HH} = 8.0$ Hz, 1H, aromatics), 8.70 (d, $J_{HH} = 8.0$ Hz, 1H, aromatics); ^{31}P NMR (162 MHz, D_2O): δ 14.0 (s).

Acknowledgment. This work was supported by the US National Institutes of Health (grants GM65307 to E.O. and AR45504 to C.T.M.), the European Commission (INCO program), the Plan Nacional and by the Plan Andaluz de Investigacion (Cod. CVI-199). J.M.S. is an American Heart Association, Midwest Affiliate, Predoctoral Fellow. J.M.W.C. is a Jean Dreyfus Boissevain Undergraduate Scholar. G.A.M. was supported by the U.S. National Institutes of Health under a Ruth L. Kirschstein National Research Service Award (grant GM-65782). A.O. is a Spanish Ministry of Science and Technology Predoctoral Fellow. We thank Carmen Tejero Extremera for technical assistance, and Roberto Docampo and Felix Ruiz, for advice on *D. discoideum* culture.

Supporting Information Available: Microanalytical and NMR data are available as Supporting Information. This material is available free of charge via the Internet at http://pubs.acs.org.

References

(1) Sambrook, P. N.; Geusens, P.; Ribot, C.; Solimano, J. A.; Ferrer-Barriendos, J.; Gaines, K.; Verbruggen, N.; Melton, M. E. Alendronate produces greater effects than raloxifene on bone density and bone turnover in postmenopausal women with low bone density: results of EFFECT (EFficacy of FOSAMAX versus EVISTA Comparison Trial) International. *J. Intern. Med.* **2004**, *255*, 503−511.

(2) Vasireddy, S.; Talwakar, A.; Miller, H.; Mehan, R.; Swinson, D. R. Patterns of pain in Paget's disease of bone and their outcomes on treatment with pamidronate. *Clin. Rheumatol.* **2003**, *22*, 376−380.

(3) Dawson, N. A. Therapeutic benefit of bisphosphonates in the management of prostate cancer-related bone disease. *Expert. Opin. Pharmacother.* **2003**, *4*, 705−716.

(4) Rosen, L. S.; Gordon, D. H.; Dugan, W. Jr.; Major, P.; Eisenberg, P. D.; Provencher, L.; Kaminski, M.; Simeone, J.; Seaman, J.; Chen, B. L.; Coleman, R. E. Zoledronic acid is superior to pamidronate for the treatment of bone metastases in breast carcinoma patients with at least one osteolytic lesion. *Cancer* **2004**, *100*, 36−43.

(5) Cromartie, T. H.; Fisher, K. J.; Grossman, J. N. The discovery of a novel site of action for herbicidal bisphosphonates. *Pesticide Biochem. Phys.* **1999**, *63*, 114−126.

(6) Cromartie, T. H.; Fisher, K. J. Method of controlling plants by inhibition of farnesyl pyrophosphate synthase. U.S. Patent 5,-756,423, May 26, 1998.

(7) van Beek, E.; Pieterman, E.; Cohen, L.; Löwik, C.; Papapoulos, S. Nitrogen-containing bisphosphonates inhibit isopentenyl pyrophosphate isomerase/farnesyl pyrophosphate synthase activity with relative potencies corresponding to their antiresorptive potencies *in vitro* and *in vivo*. *Biochem. Biophys. Res. Commun.* **1999**, *255*, 491−494.

(8) van Beek, E.; Pieterman, E.; Cohen, L.; Löwik, C.; Papapoulos, S. Farnesyl pyrophosphate synthase is the molecular target of nitrogen-containing bisphosphonates. *Biochem. Biophys. Res. Commun.* **1999**, *264*, 108−111.

(9) Keller, R. K.; Fliesler, S. J. Mechanism of aminobisphosphonate action: characterization of alendronate inhibition of the isoprenoid pathway. *Biochem. Biophys. Res. Commun.* **1999**, *266*, 560−563.

(10) Bergstrom, J. D.; Bostedor, R. G.; Masarachia, P. J.; Reszka, A. A.; Rodan, G. Mechanism of aminobisphosphonate action: characterization of alendronate inhibition of the isoprenoid pathway. *Arch. Biochem. Biophys.* **2000**, *373*, 231−241.

(11) Grove, J. E.; Brown, R. J.; Watts, D. J. The intracellular target for the antiresorptive aminobisphosphonate drugs in *Dictyostelium discoideum* is the enzyme farnesyl diphosphate synthase. *J. Bone Miner. Res.* **2000**, *15*, 971−981.

(12) Dunford, J. E.; Thompson, K.; Coxon, F. P.; Luckman, S. P.; Hahan, F. M.; Poulter, C. D.; Ebetino, F. H.; Rogers, M. J. Structure−activity relationships for inhibition of farnesyl diphosphate synthase in vitro and inhibition of bone resorption *in vivo* by nitrogen-containing bisphosphonates. *J. Pharmacol. Exp. Ther.* **2001**, *296*, 235−242.

(13) Luckman, S. P.; Hughes, D. E.; Coxon, F. P.; Graham, R.; Russell, G.; Rogers, M. J. Nitrogen-containing bisphosphonates inhibit the mevalonate pathway and prevent post-translational prenylation of GTP-binding proteins, including Ras. *J. Bone Miner. Res.* **1998**, *13*, 581−589.

(14) Fisher, J. E.; Rogers, M. J.; Halasy, J. M.; Luckman, S. P.; Hughes, D. E.; Masarachia, P. J.; Wesolowski, G.; Russell, R. G.; Rodan, G. A.; Reszka, A. A. Alendronate mechanism of action: geranylgeraniol, an intermediate in the mevalonate pathway, prevents inhibition of osteoclast formation, bone resorption, and kinase activation in vitro. *Proc. Natl. Acad. Sci. U.S.A.* **1999**, *96*, 133−138.

(15) van Beek, E.; Löwik, C.; van der Pluijm, G.; Papapoulos, S. The role of geranylgeranylation in bone resorption and its suppression by bisphosphonates in fetal bone explants *in vitro*: A clue to the mechanism of action of nitrogen-containing bisphosphonates. *J. Bone Miner. Res.* **1999**, *14*, 722−729.

(16) Montalvetti, A.; Bailey, B. N.; Martin, M. B.; Severin, G. W.; Oldfield, E.; Docampo, R. Bisphosphonates are potent inhibitors of *Trypanosoma cruzi* farnesyl pyrophosphate synthase. *J. Biol. Chem.* **2001**, *276*, 33930−33937.

(17) Sanders, J. M.; Gómez, A. O.; Mao, J.; Meints, G. A.; van Brussel, E. M.; Burzynska, A.; Kafarski, P.; González-Pacanowska, D.; Oldfield, E. 3-D QSAR investigations of the inhibition of *Leishmania major* farnesyl pyrophosphate synthase by bisphosphonates. *J. Med. Chem.* **2003**, *46*, 5171−5183.

(18) Martin, M. B.; Grimley, J. S.; Lewis, J. C.; Heath, H. T. III; Bailey, B. N.; Kendrick, H.; Yardley, V.; Caldera, A.; Lira, R.; Urbina, J. A.; Moreno, S. N.; Docampo, R.; Croft, S. L.; Oldfield, E. Bisphosphonates inhibit the growth of *Trypanosoma brucei*, *Trypanosoma cruzi*, *Leishmania donovani*, *Toxoplasma gondii*, and *Plasmodium falciparum*: A potential route to chemotherapy. *J. Med. Chem.* **2001**, *44*, 909−916.

(19) Martin, M. B.; Sanders, J. M.; Kendrick, H.; de Luca-Fradley, K.; Lewis, J. C.; Grimley, J. S.; van Brussel, E. M.; Olsen, J. R.; Meints, G. A.; Burzynska, A.; Kafarski, P.; Croft, S. L.; Oldfield, E. Activity of bisphosphonates against *Trypanosoma brucei rhodesiense*. *J. Med. Chem.* **2002**, *45*, 2904−2914.

(20) Moreno, B.; Bailey, B. N.; Luo, S.; Martin, M. B.; Kuhlenschmidt, M.; Moreno, S. N.; Docampo, R.; Oldfield, E. ^{31}P NMR of apicomplexans and the effects of risedronate on *Cryptosporidium parvum* growth. *Biochem. Biophys. Res. Commun.* **2001**, *284*, 632−637.

(21) Ghosh, S.; Chan, J. M.; Lea, C. R.; Meints, G. A.; Lewis, J. C.; Tovian, Z. S.; Flessner, R. M.; Loftus, T. C.; Bruchhaus, I.; Kendrick, H.; Croft, S. L.; Kemp, R. G.; Kobayashi, E. Effects of bisphosphonates on the growth of *Entamoeba histolytica* and *Plasmodium* species in vitro and in vivo. *J. Med. Chem.* **2004**, *47*, 175−187.

(22) Yardley, V.; Khan, A. A.; Martin, M. B.; Slifer, T. R.; Araujo, F. G.; Moreno, S. N.; Docampo, R.; Croft, S. L.; Oldfield, E. In vivo activities of farnesyl pyrophosphate synthase inhibitors against *Leishmania donovani* and *Toxoplasma gondii*. *Antimicrob. Agents Chemother.* **2002**, *46*, 929−931.

(23) Rodriguez, N.; Bailey, B. N.; Martin, M. B.; Oldfield, E.; Urbina, J. A.; Docampo, R. Radical cure of experimental cutaneous leishmaniasis by the bisphosphonate pamidronate. *J. Infect. Dis.* **2002**, *186*, 138−140.

(24) Garzoni, L. R.; Caldera, A.; Meirelles, M. N. L.; de Castro, S. L.; Meints, G.; Docampo, R.; Oldfield, E.; Urbina, J. A. Selective in vitro effects of the farnesyl pyrophosphate synthase inhibitor risedronate on *Trypanosoma cruzi*. *Intl. J. Antimicrob. Agents* **2004**, *23*, 273−285.

(25) Garzoni, L. R.; Waghabi, M. C.; Baptista, M. M.; de Castro, S. L.; Meirelles, M. N. L.; Britto, C.; Docampo, R.; Oldfield, E.; Urbina, J. A. Antiparasitic activity of risedronate in a murine model of acute Chagas' disease. *Int. J. Antimicrob. Agents* **2004**, *23*, 286−290.

(26) Wang, L.; Kamath, A.; Das, H.; Li, L.; Bukowski, J. F. Antibacterial effect of human Vγ2Vδ2 T cells in vivo. *J. Clin. Invest.* **2001**, *108*, 1349−1357.

(27) Kunzmann, V.; Bauer, E.; Feurle, J.; Weissinger, F.; Tony, H. P.; Wilhelm, M. Stimulation of $\gamma\delta$ T cells by aminobisphosphonates and induction of antiplasma cell activity in multiple myeloma. *Blood* **2000**, *96*, 384−392.
(28) Kato, Y.; Tanaka, Y.; Miyagawa, F.; Yamashita, S.; Minato, N. Targeting of tumor cells for human $\gamma\delta$ T cells by nonpeptide antigens. *J. Immunol.* **2001**, *167*, 5092−5098.
(29) Thompson, K.; Rogers, M. J. Statins prevent bisphosphonate-induced $\gamma\delta$-T-cell proliferation and activation in vitro. *J. Bone Miner. Res.* **2004**, *19*, 278−288.
(30) Sanders, J. M.; Ghosh, S.; Chan, J. M. W.; Meints, G.; Wang, H.; Raker, A. M.; Song, Y.; Colantino, A.; Burzynska, A.; Kafarski, P.; Morita, C. T.; Oldfield, E. Quantitative structure−activity relationships for $\gamma\delta$ T cell activation by bisphosphonates. *J. Med. Chem.* **2004**, *47*, 375−384.
(31) Wilhelm, M.; Kunzmann, V.; Eckstein, S.; Reimer, P.; Weissinger, F.; Ruediger, T.; Tony, H. P. $\gamma\delta$ T cells for immune therapy of patients with lymphoid malignancies. *Blood* **2003**, *102*, 200−206.
(32) Kotsikorou. E.; Oldfield, E. A quantitative structure−activity relationship and pharmacophore modeling investigation of aryl-X and heterocyclic bisphosphonates as bone resorption agents. *J. Med. Chem*. **2003**, *46*, 2932−2944.
(33) Cramer, R. D. III; Patterson, D. E.; Bunce, J. D. Recent advances in comparative molecular field analysis (CoMFA). *Prog. Clin. Biol. Res*. **1989**, *291*, 161−165.
(34) Klebe, G.; Abraham, U.; Mietzner, T. Molecular similarity indices in a comparative analysis (CoMSIA) of drug molecules to correlate and predict their biological activity. *J. Med. Chem.* **1994**, *37*, 4130−4146.
(35) *Catalyst*, version 4.8; Accelrys Inc., 9685 Scranton Rd., San Diego, CA 92121.
(36) (a) Golomb, G.; Danenberg, H. Treatment of restenosis. US Patent 6,719,998, 2004. (b) Danenberg, H.; Golomb, G. Treatment of restenosis. World Patent WO0003677, 2000. (c) Grossmann, G.; Grossmann, A.; Ohms, G.; Breuer, E.; Chen, R.; Golomb, G.; Cohen, H.; Hägele, G.; Classen, R. Solid-state NMR of bisphosphonates adsorbed on hydroxyapatite. *Magn. Reson. Chem*. **2000**, *38*, 11−16. (d) Cohen, H.; Alfer'ev, I. S.; Monkkonen, J.; Seibel, M. J.; Pinto, T.; Ezra, A.; Solomon, V.; Stepensky, D.; Sagi, H.; Ornoy, A.; Patlas, N.; Hagele, G.; Hoffman, A.; Breuer, E.; Golomb G. Synthesis and preclinical pharmacology of 2-(2-aminopyrimidinio) ethylidene-1,1-bisphosphonic acid betaine (ISA-13−1)-a novel bisphosphonate. *Pharm. Res.* **1999**, *16*, 1399−1406. (e) Patlas, N.; Golomb, G.; Yaffe, P.; Pinto, T.; Breuer, E.; Ornoy, A. Transplacental effects of bisphosphonates on fetal skeletal ossification and mineralization in rats. *Teratology* **1999**, *60*, 68−73. (f) Cohen, H.; Solomon, V.; Alfer'ev, I. S.; Breuer, E.; Ornoy, A.; Patlas, N.; Eidelman, N.; Hagele, G.; Golomb G. Bisphosphonates and tetracycline: experimental models for their evaluation in calcium-related disorders. *Pharm. Res*. **1998**, *15*, 606−613. (g) Klein, B. Y.; Ben-Bassat, H.; Breuer, E.; Solomon, V.; Golomb, G. Structurally different bisphosphonates exert opposing effects on alkaline phosphatase and mineralization in marrow osteoprogenitors. *J. Cell. Biochem*. **1998**, *68*, 186−194. (h) Alfer'ev, I. S.; Breuer, E.; Golomb, G.; Ornoy, A. Novel bisphosphonates, process for their preparation and pharmaceutical compositions containing them. World Patent WO9708178, 1997. (i) Breuer, E.; Golomb, G.; Amidon, G. L.; Alfer'ev, I. S.; Rozen, N. E.-H.; Friedman-Ezra, A. Phosphonates, bisphosphonates and pharmaceutical compositions containing them. World Patent WO9631227, 1996. (j) Cohen, H.; Breuer, E.; Chen, R.; Solomon, V.; Ornoy, A.; Patlas, N.; Pinto, T.; Golomb, G. Synthesis and evaluation of nitrogen-containing novel bisphosphonates for calcium-related disorders. *Pharm. Res*. **1996**, *13*, s-139. (k) Alfer'ev, I. S.; Mikhalin, N. V. Reactions of vinylidenediphosphonic acid with nucleophiles 5. Addition of heterocyclic amines and trimethylamine to vinylidenediphosphonic acid. *Russ. Chem. Bull.* **1995**, *44*, 1528−1530. (l) Alfer'ev, I. S.; Mikhalin, N. V.; Novikova, V. M.; Kozlov, V. A. Substituted ammonioethylidene-1,1-diphosphonic acids with immunosuppressant activity. Russian Patent SU1089953, 1995.
(37) van Beek, E. R.; Löwik, C. W. G. M.; Ebetino, F. H.; Papapoulos, S. E. Binding and antiresorptive properties of heterocycle-containing bisphosphonate analogs: Structure−activity relationships. *Bone* **1998**, *23*, 437−442.
(38) Gaussian 03, Revision C.02, Frisch, M. J.; Trucks, G. W.; Schlegel, H. B.; Scuseria, G. E.; Robb, M. A.; Cheeseman, J. R.; Montgomery, Jr., J. A.; Vreven, T.; Kudin, K. N.; Burant, J. C.; Millam, J. M.; Iyengar, S. S.; Tomasi, J.; Barone, V.; Mennucci, B.; Cossi, M.; Scalmani, G.; Rega, N.; Petersson, G. A.; Nakatsuji, H.; Hada, M.; Ehara, M.; Toyota, K.; Fukuda, R.; Hasegawa, J.; Ishida, M.; Nakajima, T.; Honda, Y.; Kitao, O.; Nakai, H.; Klene, M.; Li, X.; Knox, J. E.; Hratchian, H. P.; Cross, J. B.; Bakken, V.; Adamo, C.; Jaramillo, J.; Gomperts, R.; Stratmann, R. E.; Yazyev, O.; Austin, A. J.; Cammi, R.; Pomelli, C.; Ochterski, J. W.; Ayala, P. Y.; Morokuma, K.; Voth, G. A.; Salvador, P.; Dannenberg, J. J.; Zakrzewski, V. G.; Dapprich, S.; Daniels, A. D.; Strain, M. C.; Farkas, O.; Malick, D. K.; Rabuck, A. D.; Raghavachari, K.; Foresman, J. B.; Ortiz, J. V.; Cui, Q.; Baboul, A. G.; Clifford, S.; Cioslowski, J.; Stefanov, B. B.; Liu, G.; Liashenko, A.; Piskorz, P.; Komaromi, I.; Martin, R. L.; Fox, D. J.; Keith, T.; Al-Laham, M. A.; Peng, C. Y.; Nanayakkara, A.; Challacombe, M.; Gill, P. M. W.; Johnson, B.; Chen, W.; Wong, M. W.; Gonzalez, C.; Pople, J. A.; Gaussian, Inc., Wallingford, CT, 2004.
(39) Besler, B. H.; Merz, K. M.; Kollman, P. A. Atomic charges derived from semiempirical methods. *J. Comput. Chem*. **1990**, *11*, 431−439.
(40) Singh, U. C.; Kollman, P. A. An approach to computing electrostatic charges for molecules. *J. Comput. Chem*. **1984**, *5*, 129−145
(41) Miyaura, N.; Yanagi, T.; Suzuki, A. The palladium-catalyzed cross-coupling reaction of phenylboronic acid with haloarenes in the presence of bases. *Synth. Commun*. **1981**, *11*, 513−519.
(42) Krapcho, A. P.; Ellis, M. Synthesis of regioisomeric difluoro- and 8-chloro-9-fluorobenz[*g*]isoquinoline-5,10-diones and S_NAr displacements studies by diamines: bis(aminoalkyl)aminobenz[*g*]-isoquinoline-5, 10-diones. *J. Fluorine Chem*. **1998**, *90*, 139−147.
(43) Zhang, L.; Liang, F.; Sun, L.; Hu, Y.; Hu, H. A novel and practical synthesis of 3-unsubstituted indolizines. *Synthesis* **2000**, 1733−1737.
(44) Harel, Z.; Kovalevski-Liron, E.; Lidor-Hadas, R.; Lifshitz-Liron, R. Use of certain diluents for making bisphosphonic acids. World Patent WO03097655, November 27, 2003.
(45) Rogers, M. J.; Watts, D. J.; Russell, R. G.; Ji, X.; Xiong, X.; Blackburn, G. M.; Bayless, A. V.; Ebetino, F. H. Inhibitory effects of bisphosphonates on growth of amoebae of the cellular slime mold *Dictyostelium discoideum*. *J. Bone Miner. Res.* **1994**, *9*, 1029−1039.
(46) van Beek, E. R.; Cohen, L. H.; Leroy, I. M.; Ebetino, F. H.; Löwik, C. W.; Papapoulos, S. E. Differentiating the mechanisms of antiresorptive action of nitrogen containing bisphosphonates. *Bone* **2003**, *33*, 805−11.

JM040209D